Neuron
Article

C. elegans TRP Family Protein TRP-4 Is a Pore-Forming Subunit of a Native Mechanotransduction Channel

Lijun Kang,[1,4] Jingwei Gao,[1,2,4] William R. Schafer,[3] Zhixiong Xie,[2] and X.Z. Shawn Xu[1,*]
[1]Life Sciences Institute and Department of Molecular and Integrative Physiology, University of Michigan, Ann Arbor, MI 48109, USA
[2]College of Life Sciences, Wuhan University, Wuhan, Hubei 430072, China
[3]Cell Biology Division, MRC Laboratory of Molecular Biology, Cambridge CB2 0QH, UK
[4]These authors contributed equally to this work
*Correspondence: shawnxu@umich.edu
DOI 10.1016/j.neuron.2010.06.032

SUMMARY

Mechanotransduction channels mediate several common sensory modalities such as hearing, touch, and proprioception; however, very little is known about the molecular identities of these channels. Many TRP family channels have been implicated in mechanosensation, but none have been demonstrated to form a mechanotransduction channel, raising the question of whether TRP proteins simply play indirect roles in mechanosensation. Using *Caenorhabditis elegans* as a model, here we have recorded a mechanosensitive conductance in a ciliated mechanosensory neuron in vivo. This conductance develops very rapidly upon mechanical stimulation with its latency and activation time constant reaching the range of microseconds, consistent with mechanical gating of the conductance. TRP-4, a TRPN (NOMPC) subfamily channel, is required for this conductance. Importantly, point mutations in the predicted pore region of TRP-4 alter the ion selectivity of the conductance. These results indicate that TRP-4 functions as an essential pore-forming subunit of a native mechanotransduction channel.

INTRODUCTION

The activity of mechanosensitive channels has been detected in diverse cell types, including both excitable and nonexcitable cells (Gillespie and Walker, 2001). These channels can be activated by a variety of mechanical stimuli, ranging from sound to pressure, stretch, and gravity (Christensen and Corey, 2007; Gillespie and Walker, 2001). In the nervous system, several sensory modalities such as hearing, touch, and proprioception are believed to be mediated by this type of channels (Christensen and Corey, 2007; Gillespie and Walker, 2001). It has been proposed that these channels are directly gated by force to transduce mechanical stimuli into electrical signals, thereby acting as the transduction channels in mechanosensation (Christensen and Corey, 2007; Gillespie and Walker, 2001).

Despite their prevalence in diverse tissues and organisms, very little is known about the genes encoding mechanotransduction channels in metazoans (Christensen and Corey, 2007). The stretch-sensitive Msc channels found in bacteria appear to be absent in the animal kingdom (Gillespie and Walker, 2001; Kung and Blount, 2004). Thus far, merely two types of proteins have been demonstrated to form mechanotransduction channels in metazoans: the touch-sensitive ENaC family Na^+ channel MEC-4/MEC-10 in *C. elegans* and the stretch-sensitive two-pore-domain K^+ channels TREK-1/TRAAK in mammals (Honore et al., 2006; O'Hagan et al., 2005). The molecular identities of the vast majority of mechanotransduction channels, however, remain elusive (Christensen and Corey, 2007; Sharif-Naeini et al., 2008).

TRP (transient receptor potential) channels were first identified in *Drosophila* and later found to constitute a conserved superfamily of cation channels found in nearly all eukaryotes (Montell, 2005; Montell and Rubin, 1989). TRP family channels have recently emerged as the leading candidates for mechanotransduction channels (Christensen and Corey, 2007; Sharif-Naeini et al., 2008). Among the seven TRP subfamilies (Montell, 2005), nearly every subfamily has members that have been implicated in mechanosensation. These include TRPC (TRPC1, TRPC5, and TRPC6), TRPV (TRPV1, TRPV2, TRPV4, OSM-9, OCR-2, NAN, and IAV), TRPM (TRPM4 and TRPM7), TRPN (TRPN1/TRP-4/NOMPC), TRPA (TRPA1 and Painless), and TRPP (TRPP2/PKD2), as well as the more distantly related Yvc1/TRPY1 (Christensen and Corey, 2007; Gottlieb et al., 2008; Sharif-Naeini et al., 2008). However, a large body of conflicting results has been reported to argue against a direct role of many of these candidates in mechanosensation (Christensen and Corey, 2007; Sharif-Naeini et al., 2008; Yin and Kuebler, 2010). In particular, there is no evidence showing that any of these TRP proteins is mechanically gated and forms the pore of a transduction channel (Christensen and Corey, 2007). Thus, the question arises as to whether TRP channels merely play an indirect role in mechanosensation; for example, they may act downstream to amplify or modulate the signal from the transduction channel or other components in the pathway (e.g., Gq/PLCβ and PLA2) (Christensen and Corey, 2007; Gottlieb et al., 2008; Mederos

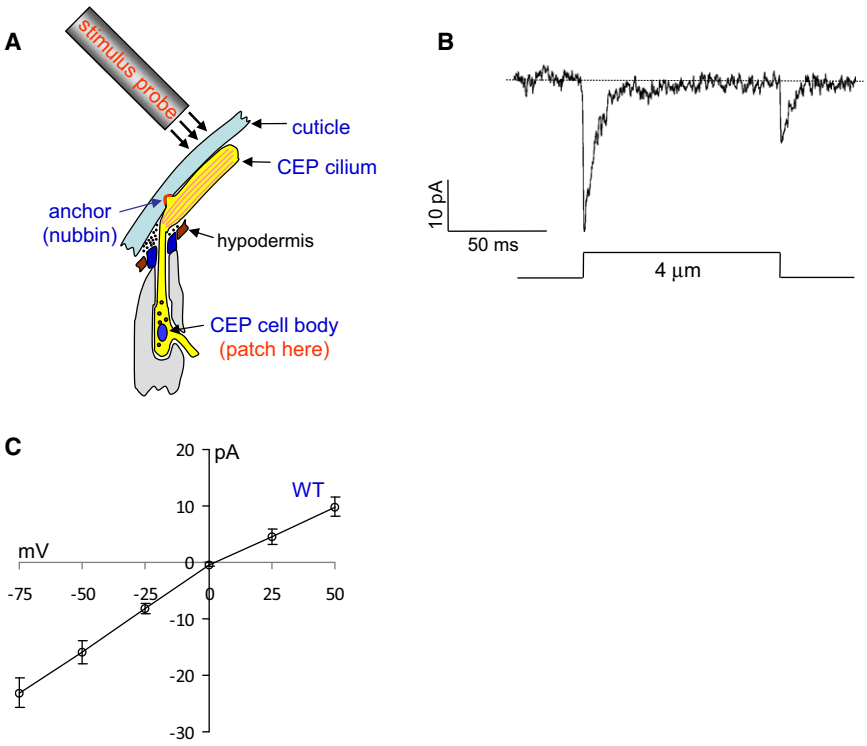

Figure 1. In Vivo Patch-Clamp Recording of Mechanoreceptor Currents in the Dopamine Neuron CEP

(A) A schematic illustrating the morphology of CEP (Perkins et al., 1986). A glass probe (2 μm in diameter) driven by a piezo actuator was used to deliver mechanical stimuli toward the CEP cilium (not drawn to scale).

(B) MRCs in CEP evoked by a 4 μm stimulus. CEP cell body was voltage clamped at −75 mV. The dotted line in this trace and all other traces in this paper denotes the baseline (zero current). Most, if not all, worm neurons particularly head sensory neurons are known to be nearly isopotential (voltage is quite uniform throughout the neuron), and thus voltage attenuation (space clamp) is minimal (Goodman et al., 1998).

(C) I-V relations of MRCs in CEP. Peak current values were used here and throughout the paper. n = 6.

y Schnitzler et al., 2008; Sharif-Naeini et al., 2008; Watanabe et al., 2003).

One main challenge lies in the relative difficulty of functionally reconstituting mechanotransduction channels in heterologous systems. Unlike voltage-, ligand-, or temperature-gated channels, the proper function of many mechanotransduction channels probably requires tethering of the channel to the cytoskeleton and/or extracellular matrix, as well as the function of auxiliary subunits, a setting that is difficult to recapitulate in heterologous systems (Christensen and Corey, 2007; Gillespie and Walker, 2001; Gottlieb et al., 2008).

Here we sought to attack this question in vivo. We resorted to the nematode *C. elegans*, a popular genetic model organism that encodes 17 TRP family genes covering all of the seven TRP subfamilies and possesses mechanosensory modalities such as touch, proprioception, and osmosensation (Kahn-Kirby and Bargmann, 2006; Xiao and Xu, 2009). By combining in vivo patch-clamp recording and molecular genetic manipulation, we demonstrate that the TRPN channel TRP-4 acts as an essential pore-lining subunit of a native mechanosensory transduction channel. Thus, TRP family channels can play a direct role in mechanosensation.

RESULTS

Mechanical Stimuli Evoke Mechanoreceptor Currents in CEP

We focused on CEP (cephalic neuron), a mechanosensory dopamine neuron with a sensory cilium located at the nose tip of the worm (Sawin et al., 2000). Notably, the CEP cilium is anchored to the cuticle through a small nubbin (Perkins et al., 1986) (Figure 1A). Deflection of the cuticle by mechanical stimuli such as pressure/touch would lead to deflection of the cilium. Under laboratory conditions, this neuron can sense mechanical pressure imposed by bacterial particles (i.e., food source for worms) during locomotion and foraging (Sawin et al., 2000). Activation of CEP neurons presumably leads to release of dopamine, an inhibitory neurotransmitter for locomotion (Sawin et al., 2000). Consequently, worms reduce their locomotion speed to facilitate feeding, a phenomenon that was first described by Sawin et al. as the basal slowing response (Sawin et al., 2000). As previously reported (Sawin et al., 2000), dopamine deficient mutants (e.g., *cat-2*) lacked this behavioral response (Figure S1A).

As a first step, we developed a protocol to record the activity of CEP in response to mechanical stimuli by whole-cell patch-clamp recording (Figure 1A). We carefully exposed the cell body of CEP to recording pipettes by removing a small piece of cuticle in the head while keeping intact the nose tip where the CEP cilium is housed. A glass probe driven by a piezo actuator was used to deliver mechanical stimuli toward the CEP cilium in a rapid manner with precision (Figure 1A). To facilitate recording, we expressed a fluorescent protein as a transgene in CEP to mark its cilium and cell body.

Mechanical stimuli evoked a rapidly adapting mechanoreceptor current (MRC) in CEP (Figure 1B). Removal of the stimulus also elicited a similar current in CEP, though with a smaller amplitude (Figure 1B). Eliminating Cl^- from the pipette solution did not affect the reversal potential (Figure S1B), consistent with the view that these currents are carried by cation channels (see below). The presence of both "on" and "off" MRCs is similar to that observed in PLM (posterior lateral microtubule cell), a non-ciliated neuron that detects posterior body touch (O'Hagan et al., 2005). However, unlike the ENaC channel-mediated MRCs in PLM that are Na^+ selective (O'Hagan et al., 2005), the MRCs in CEP were nonselective with a reversal potential close to 0 mV

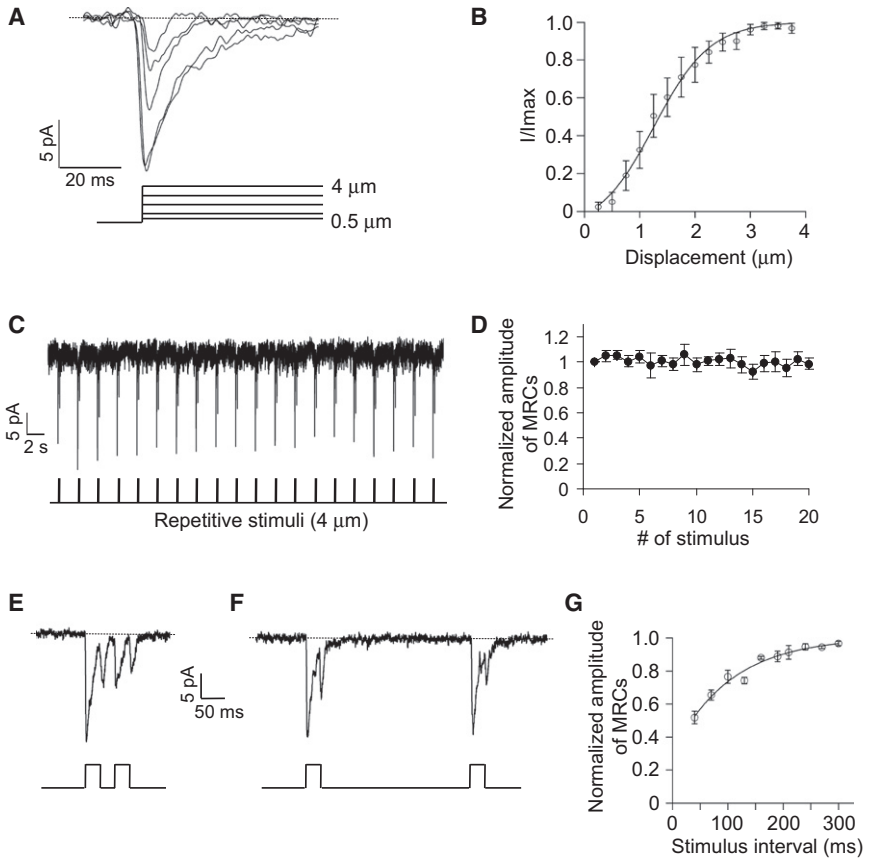

Figure 2. The Amplitude of MRCs Is Stimulus-Strength Dependent and They Do Not Desensitize to Repetitive Stimuli with Long Intervals

(A and B) The amplitude of MRCs is stimulus-strength dependent. Mechanical stimuli of varying displacement were used to stimulate CEP. Shown in (A) are sample traces recorded from a CEP neuron in response to 0.5, 1, 2, 3, and 4 μm of displacement. Each trace was averaged from four sweeps. I/Imax values were plotted against displacement in (B), and the data were fit with a Boltzmann function: $I/I_{max} = 1/\{1 + \exp[-(X - X_{1/2})/X_{slope}]\}$, where I denotes current amplitude and X represents displacement. n = 6.

(C and D) MRCs in CEP do not desensitize to repetitive stimuli with long intervals. Repetitive stimuli (4 μm) were applied to CEP neurons for 50 times with an interval of 2 s between each stimulus. Shown in (C) is a sample trace of the first 20 responses, and the data are summarized in (D). n = 9.

(E–G) MRCs in CEP show desensitization to repetitive stimuli with short intervals. (E) Two consecutive stimuli (4 μm) with a short interval (30 ms) were applied to CEP. The amplitude of MRCs evoked by the second stimulus was greatly reduced compared to that triggered by the first stimulus, indicating desensitization.

(F) However, no such desensitization was observed in CEP when we applied repetitive stimuli with a long interval (300 ms). Traces shown in (E) and (F) were from the same neuron.

(G) Data summary. n = 4. Error bars represent SEM.

(Figure 1C). In addition, CEP MRCs appeared to be insensitive to amiloride (Figures S1C–S1E). By contrast, we found that as previously reported (O'Hagan et al., 2005), the ENaC-mediated MRCs in PLM were blocked by 200 μM amiloride (Figures S1F–S1H). Furthermore, the I-V relationship of CEP conductance was nearly linear (Figure 1C), another feature distinct from that observed in PLM (O'Hagan et al., 2005). These results indicate that MRCs in CEP are probably mediated by a distinct class of mechanotransduction channels. As the "on" MRC in CEP is more robust than the "off" MRC, we decided to focus our efforts on the "on" MRC.

The Amplitude of MRCs in CEP Depends on the Strength of Mechanical Stimuli

The amplitude of MRCs in CEP is stimulus-strength dependent (Figures 2A and 2B). A displacement of 0.5 μm was sufficient to evoke a MRC in CEP, which saturated around 3 μm (Figures 2A and 2B). Thus, CEP can sense submicrometer range of deflection. This sensitivity may allow CEP to detect mechanical attributes from bacterial particles whose size is usually about 1 μm.

MRCs in CEP Do Not Desensitize to Repeated Stimuli with Long Intervals

To test whether MRCs undergo desensitization, we applied repetitive stimuli to CEP. Repetitive stimulation of CEP (>20 times) at an interval of 2 s elicited MRCs with similar amplitude, indicating that under such a condition these currents did not desensitize (Figures 2C and 2D). Interestingly, CEP did show desensitization to repetitive stimuli with short intervals (Figures 2E–2G). Under this condition, the amplitude of MRCs evoked by the second stimulus was greatly reduced compared with that triggered by the first stimulus (Figure 2E). However, such a phenomenon was not observed when we extended the stimulus interval (Figures 2F and 2G). The exact mechanism underlying this observation is not clear. These results demonstrate that, though MRCs in CEP rapidly adapt, they do not appear to desensitize to repeated stimuli with long intervals.

MRCs in CEP Show Rapid Activation Kinetics and Short Latency

One of the hallmarks of mechanically gated channels is that the kinetics of channel activation should depend on the strength of the stimulus (Christensen and Corey, 2007). Namely, the stronger the stimulus is, the faster the channel opens, as larger forces lower the energy barrier to channel opening more efficiently. We found that the activation kinetics of MRCs in CEP was very rapid with a time constant reaching the range of microseconds at saturating stimulus levels (650 ± 90 μs at 4 μm). More importantly, this time constant reduced with increasing stimulus strength (Figure 3A), indicating that the activation kinetics of the transduction channel in CEP depends on the strength of the stimulus.

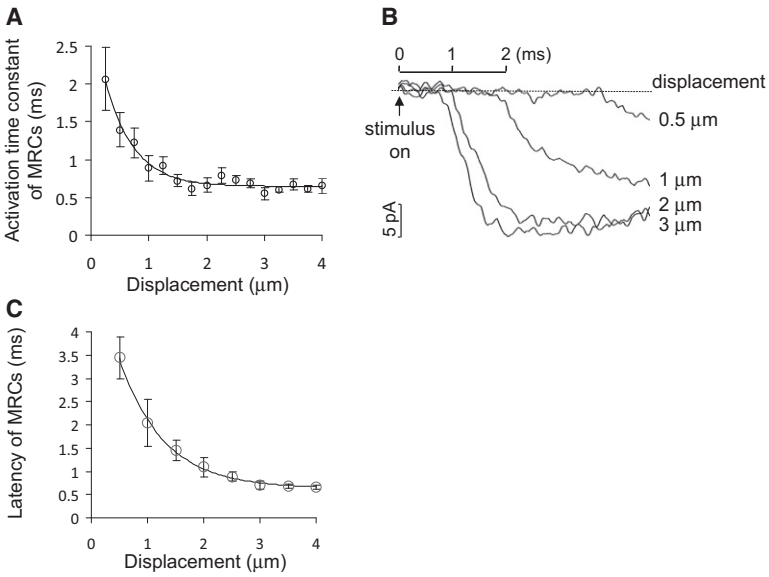

Figure 3. MRCs in CEP Show Rapid Activation Kinetics and Short Latency

(A) The activation kinetics of MRCs becomes faster with increasing stimulus strength, reaching the microsecond range. The activation time constants of MRCs were plotted as a function of displacement, and the solid line represents a single exponential fit to the data. n = 6.

(B and C) The latency of MRCs reduces with increasing stimulus strength, reaching the microsecond range. Shown in (B) are sample traces, and the arrow indicates the onset of the stimulus. Latency values were plotted against displacement in (C), and the solid line represents a single exponential fit to the data. n = 6.

Another key feature of mechanically gated channels is that the latency of channel activation should be shorter than known second-messenger pathways, usually less than 5 ms (Christensen and Corey, 2007). This makes it unlikely the involvement of second-messengers in channel gating. The latency of MRCs in CEP decreased with increasing stimulus strength, reaching the microsecond range at saturating stimulus levels (670 ± 40 μs at 4 μm; Figures 3B and 3C). The short latency and rapid activation kinetics of MRCs in CEP suggest that the underlying transduction channel is mechanically gated.

Single-Channel Conductance

We then estimated the single channel conductance of the transduction channel through nonstationary noise analysis of MRCs in CEP (Figures 4A and 4B), as it is technically difficult to record single channel events of this type of channels by excised patch. We found that the single channel current was 1.3 ± 0.1 pA (n = 7) at −75 mV. Thus, the single channel conductance (γ) appeared to be 16 ± 2 pS. This analysis also estimated that there was an average of 21 ± 2 functional transduction channels in each recorded CEP neuron.

Adaptation Extends the Dynamic Range of CEP Mechanosensitivity

Last, we characterized the adaptation of MRCs in CEP. Adaptation allows sensory receptors to adjust their response such that they can maintain their sensitivity to new stimuli in the presence of the existing stimulus (LeMasurier and Gillespie, 2005). It is a critical mechanism for sensory receptors to extend their dynamic range of response (LeMasurier and Gillespie, 2005). This feature is observed in several types of sensory receptors such as photoreceptors and hair cells in vertebrates (LeMasurier and Gillespie, 2005). To test this, we first applied a testing stimulus to CEP to record its initial response (Figure 5A). We then delivered an adapting stimulus followed by another testing stimulus on top of the adapting stimulus to examine the responsiveness of CEP (Figure 5A). Though CEP quickly adapted to the adapting stimulus, it can further respond to additional stimuli in the presence of the adapting stimulus (Figure 5A). As a consequence, the stimulus-response curve shifted to the right (Figure 5B). This feature greatly extends the dynamic range of response of CEP.

TRP-4 Is Required for MRCs in CEP

Having characterized MRCs in CEP, we then asked what channels carry this type of currents. TRP-4, a TRPN subfamily channel, appears to be a promising candidate for a number of reasons. TRP-4 is expressed in mechanosensory neurons, including CEP, and is localized to the cilium of CEP where

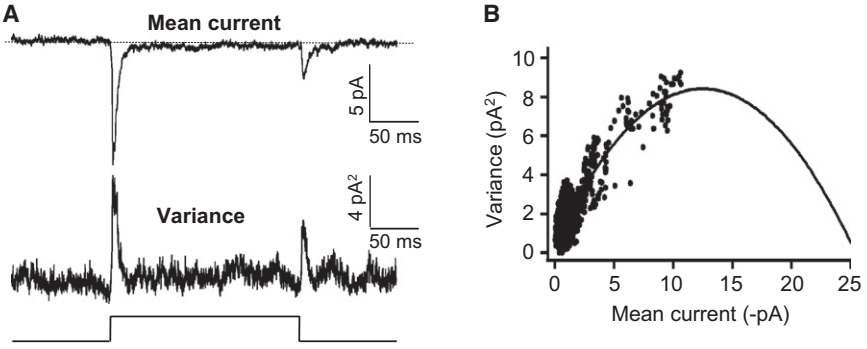

Figure 4. Nonstationary Noise Analysis

(A and B) Nonstationary noise analysis of MRCs. Shown in (A) are the ensemble average MRC trace (top) and the variance trace (bottom) from a CEP neuron in response to 50 repetitive stimuli (1 μm) with an interval of 2 s between each stimulus, a condition under which desensitization to repetitive stimuli did not occur (Figures 2C and 2D). The variance values were plotted against mean current, and the data were fit with the equation: $\sigma^2(I) = iI - I^2/N$, where σ^2 is the variance, i represents the single channel current, and N indicates the number of channels available for activation (see Experimental Procedures for details). For the cell shown in (B), i = 1.2 pA and N = 23.

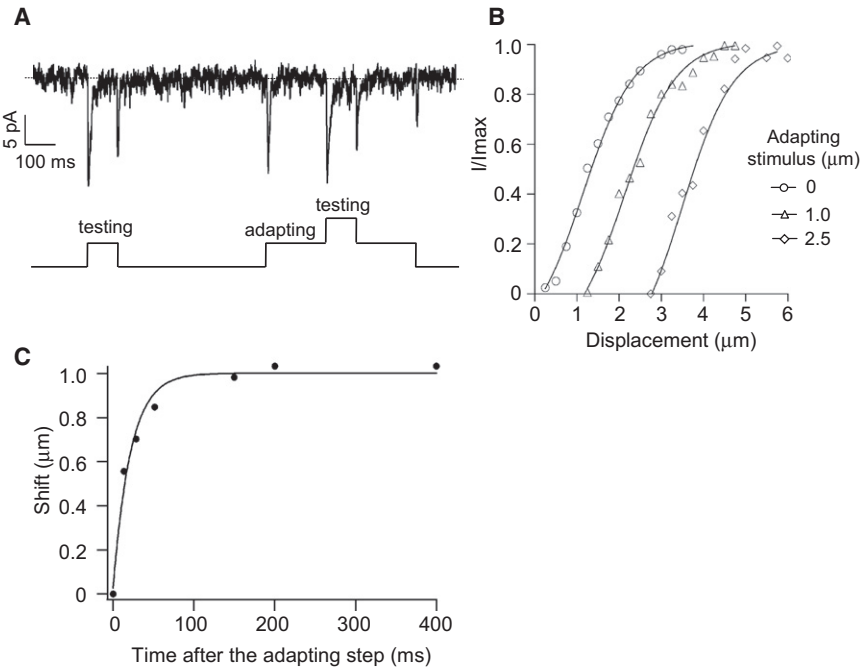

Figure 5. Adaptation Extends the Dynamic Range of CEP Mechanosensitivity

(A and B) Adaptation extends the dynamic range of response in CEP. Shown in (A) is a sample trace of a CEP neuron in response to a series of testing and adapting stimuli (1 μm). The I/Imax values under different adapting stimulus strength were plotted against displacement, and the data were fit with a Boltzmann function: $I/I_{max} = 1/(1 + \exp\{-[(X - X_0) - X_{1/2}]/X_{slope}\})$, where I denotes current amplitude, X represents displacement, and X_0 indicates adapting displacement. The actual shift of the stimulus-response curve estimated based on $\Delta X_{1/2}$ is 1.0 and 2.4 μm under 1.0 and 2.5 μm of adapting displacement, respectively. Each curve represents data points from at least three cells.

(C) Time course of the adaptive shift of the stimulus-response curve. Unlike in (B) where testing pulses were applied at a fixed time point (200 ms) after the onset of adapting pulses of varying strength, here testing pulses were delivered at varying time points (0–400 ms) after the onset of a adapting pulse of fixed strength (1 μm). $X_{1/2}$ value under each condition was calculated as described in (B). By doing so, the actual shift of the stimulus-response curve (i.e., $\Delta X_{1/2}$ values) was obtained for each condition (time point), and this value was plotted against time points as shown in (C). n = 7.

mechanotransduction presumably occurs (Li et al., 2006; Walker et al., 2000). *trp-4* mutant worms are defective in mechanosensation such as the basal slowing response and proprioception (Li et al., 2006), and show defective calcium transients in some TRP-4 neurons (e.g., the DVA proprioceptive neuron and CEP) (Kindt et al., 2007a; Li et al., 2006). In addition, both the zebra fish and fly homologs of TRP-4 have been implicated in mechanosensation (Sidi et al., 2003; Walker et al., 2000). For example, extracellular recordings show that the fly TRP-4 homolog TRPN1/NOMPC is required for one of the two components of trans-epithelial currents induced by bristle displacement in bristle organs (Walker et al., 2000). However, because of some technical constraints, it has not been possible to directly record the mechanosensory neuron of fly bristle organs by patch-clamp. Thus, it remains unclear whether TRPN1/NOMPC forms the pore of a mechanotransduction channel in these organs (Christensen and Corey, 2007; Gillespie and Walker, 2001).

The ability to record MRCs in CEP by patch-clamp offers us a unique opportunity to test whether TRP-4 can form a mechanotransduction channel in vivo. We thus recorded CEP in *trp-4* mutant worms and found that mutant worms lacked MRCs (Figure 6A–6D). Like other neurons, CEP also expresses voltage-sensitive currents such as K^+ currents (Davies et al., 2003), but these currents appeared normal in *trp-4* mutant worms, indicating that *trp-4* mutations do not globally affect ionic currents (Figures S2A–S2C). Behaviorally, we confirmed that as previously reported (Li et al., 2006), mutant worms lacked the basal slowing response (Figure 6E). Expression of wild-type *trp-4* cDNA in CEP under a dopamine neuron-specific promoter rescued MRCs in CEP (Figures 6C and 6D), as well as the basal slowing behavioral response (Figure S1). As a control, expression of *ocr-2* cDNA yielded no rescuing effect on either phenotype (Figures 6D and 6E), though this cDNA can rescue the osmotic and octanol avoidance defects of *ocr-2* mutant worms (Figures S2D and S2E). In addition, as was the case with wild-type worms, the I-V relationship of MRCs in rescued worms was nearly linear with a reversal potential close to 0 (Figures 6F and 6G). The response latency and activation kinetics of MRCs in rescued worms (latency: 610 ± 110 μs, activation time constant: 590 ± 40 μs at 4 μm, n = 6) were also very similar to those in wild-type worms. These results demonstrate that TRP-4 is required for MRCs in CEP.

However, an essential role of TRP-4 for MRCs in CEP does not provide evidence that TRP-4 forms the transduction channel that carries MRCs in this neuron. Many alternative models exist. For example, TRP-4 may be an essential auxiliary subunit of the transduction channel complex; TRP-4 may also be required for the expression, assembly, and/or targeting of the transduction channel. To demonstrate that a protein forms the pore of an ion channel that carries a defined conductance, one of the most commonly used approaches is to show that the ion selectivity of the conductance can be altered by manipulating the residues in the predicted pore region of the candidate protein (Hille, 2001). Thus, we decided to apply this approach to TRP-4. One challenge is that, while it is relatively easy to alter the ion selectivity of selective channels (e.g., Na^+ and K^+ channels) by rendering them nonselective, it is generally more difficult to do so with nonselective channels (most TRP channels are nonselective).

Mutations Outside of the Predicted Pore Region of TRP-4 Do Not Alter the Ion Selectivity of the Transduction Channel

TRP family channels are structurally and evolutionarily related to voltage-gated K^+ channels and contain six putative

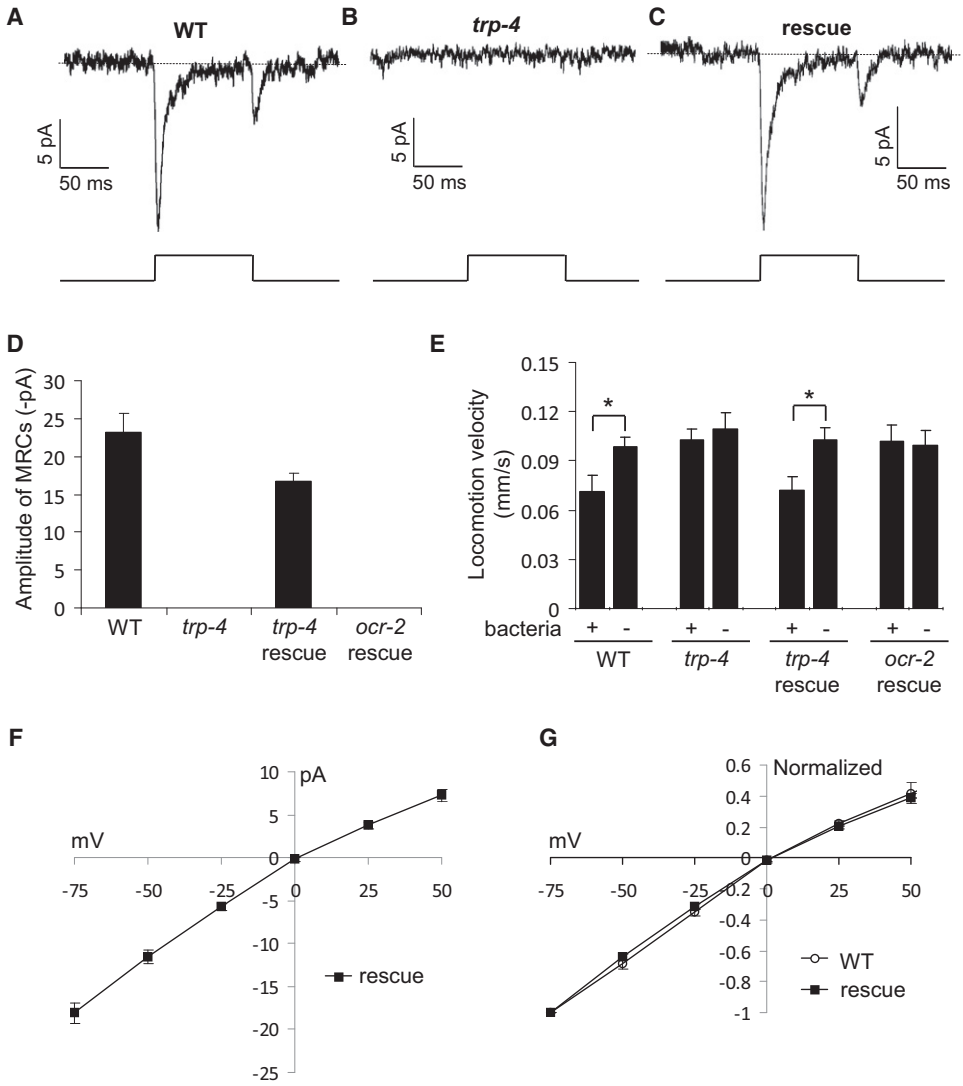

Figure 6. TRP-4 Is Required for MRCs in CEP

(A and B) TRP-4 is required for MRCs in CEP. (A) Wild-type. (B) No MRC was detected in CEP of *trp-4(sy695)* mutant worms in response to a saturating stimulus (4 μm). *sy695* is a null allele of *trp-4* (Li et al., 2006).

(C) Transgenic expression of wild-type *trp-4* cDNA in CEP under the dopamine neuron-specific promoter *dat-1* (Lints and Emmons, 1999) rescues MRCs in *trp-4 (sy695)* mutant worms.

(D) Bar graph summarizing the data in (A–C). *ocr-2* cDNA under the *dat-1* promoter failed to rescue MRCs in CEP. $n \geq 6$.

(E) *trp-4* mutant worms are defective in the basal slowing behavioral response, and this phenotype can be rescued by transgenic expression of wild-type *trp-4* cDNA, but not *ocr-2* cDNA. *ocr-2* cDNA can rescue the osmotic and octanol avoidance defects of *ocr-2* mutants (see Figures S2D and S2E). $n \geq 10$. *$p < 0.05$ (t test).

(F) I-V relations of CEP MRCs recorded from rescued worms. n = 7.

(G) I-V relations of CEP MRCs recorded from rescued worms and wild-type worms are nearly identical.

transmembrane domains with both the N and C termini in the cytoplasm and a putative pore region between the fifth (S5) and sixth (S6) transmembrane segments (Nilius and Voets, 2005; Ramsey et al., 2006; Venkatachalam and Montell, 2007). We examined the putative pore region in the linker area between S5 and S6 in TRP-4. By analogy to K^+ channels, the pore of TRP-4 would comprise a pore helix followed by a selectivity filter (Figure 7A) (Owsianik et al., 2006). As TRP family channels are cation channels, we focused on the negatively charged residues D and E (Figure 7A). We mutated all of the D and E residues in the predicted pore region (Figure 7A). As a control, we also mutated nearly all of the D and E residues outside of the predicted pore region but within the linker area between S5 and S6 (Figure 7A). All of the constructs harboring point mutations were expressed in CEP as a transgene in the *trp-4* mutant background using a dopamine neuron-specific promoter, and the transgenic worms were then tested for MRCs in CEP and also for the basal slowing behavioral response (Figures 7B–7G).

MRCs recorded from both wild-type worms and *trp-4* mutant worms rescued by a wild-type *trp-4* transgene displayed a nearly linear I-V relationship with a reversal potential around +1.5 mV (Figures 6F, 6G, and 7G). This indicates that the transduction channel is nonselective, exhibiting a slightly higher permeability to Na^+ than to Cs^+ (P_{Cs^+}/P_{Na^+} = 0.94; Na^+ and Cs^+ were the primary cations in the bath and pipette solution, respectively). For technical reasons, we were unable to determine the calcium permeability (Experimental Procedures). Similarly, MRCs recorded from both the DED$^{1711-3}$AAA and E^{1716}A mutants exhibited a reversal potential indistinguishable from that observed in wild-type (Figures 7D and 7G), demonstrating that these residues are not critical for determining the ion selectivity of the transduction channel (Figure 7A). This result is consistent with the prediction that these residues are not part of the channel pore. E^{1728}K, a point mutation in the predicted pore helix (Figure 7A), also did not affect the reversal potential (Figures 7D and 7G), supporting the view that pore helix residues do not have a major effect on ion selectivity.

Mutations in the Predicted Pore Region of TRP-4 Alter the Biophysical Properties of the Transduction Channel, Including Its Ion Selectivity

Interestingly, EPD$^{1739-41}$QPN and EPD$^{1739-41}$APA, two mutants that affect residues in the putative selectivity filter (Figure 7A), shifted the reversal potential to the left by 14 mV and 12 mV, respectively (Figures 7E and 7G). Thus, these two point mutations reversed the preference of the transduction channel toward Cs^+ and Na^+ and rendered it more permeable to Cs^+ than to Na^+ (P_{Cs^+}/P_{Na^+} = 1.7 for EPD$^{1739-41}$QPN), indicating an important role for the residues E^{1739} and/or D^{1741} in regulating the ion selectivity of the transduction channel. In addition, unlike wild-type TRP-4 that displaced a nearly linear I-V relationship, these two mutant channels appeared to be a bit inwardly rectifying (Figure 7E), revealing that these residues also affect channel rectification. As both mutant forms of TRP-4 preserved much of the channel function, they rescued the basal slowing behavioral response (Figure 7C). If E^{1739} and D^{1741} are indeed important for controlling ion selectivity, more drastic mutations of these two residues may render TRP-4 nonfunctional. To test this, we mutated E^{1739} and D^{1741} to the positively charged residue K (EPD$^{1739-41}$KPK). Consistent with a critical role of these residues, the EPD$^{1739-41}$KPK mutation abrogated the function of TRP-4, since no MRC can be detected in CEP (Figures 7B and 7E, and see below). As expected, this transgene also failed to rescue the basal slowing behavioral response (Figure 7C). These results demonstrate that mutations in the predicted pore region of TRP-4 either abolished the function of or altered the biophysical properties of the transduction channel in CEP, including its ion selectivity.

Encouraged by the above results, we generated two additional mutant forms of TRP-4: EPD$^{1739-41}$AAA and EPD$^{1739-41}$GGG, both of which mutated three residues in the putative selectivity filter (Figure 7A). These two mutations shifted the reversal potential of MRCs to the left by 27 mV (EPD$^{1739-41}$GGG) and 26 mV (EPD$^{1739-41}$AAA), respectively (Figures 7F and 7G), a greater shift than that caused by EPD$^{1739-41}$QPN and EPD1739-42APA. Thus, the permeability of the transduction channel to Cs^+ is further increased (P_{Cs^+}/P_{Na^+} = 2.9 for EPD$^{1739-41}$GGG). We also observed that the I-V relations of these two mutants were inwardly rectifying (Figure 7F), a feature distinct from that observed in wild-type worms. This indicates that these two mutations also altered the rectification of the transduction channel. Taken together, our results showed that TRP-4 was required for MRCs in CEP, and that point mutations in the predicted pore region of TRP-4 either abrogated the activity or altered the biophysical properties, particularly the ion selectivity of MRCs in CEP. Thus, TRP-4 appears to be an essential pore-forming subunit of the mechanosensory transduction channel in CEP.

A Pore-Dead Mutant Form of TRP-4 Blocks the Wild-Type Transduction Channel In Vivo

To gather further evidence, we reasoned that if TRP-4 is indeed a pore-forming subunit of the transduction channel, then point mutations disrupting the pore function of TRP-4 should not only render the mutant channel nonfunctional, but also should block the wild-type channel in a dominant-negative manner. This logic is based on the fact that TRP family proteins function as multimeric channels (Strubing et al., 2001; Xu et al., 1997). To test this, we crossed the transgene expressing the "pore-dead" mutant EPD$^{1739-41}$KPK into the wild-type background. We found that wild-type worms expressing EPD$^{1739-41}$KPK showed almost no MRCs in CEP (Figures 7H and 7I), indicating a nearly complete blockade of MRCs by this mutant form of TRP-4. Remarkably, these "wild-type" worms lacked the basal slowing response and behaved just like *trp-4* mutant worms (Figure 7J). These data provide further evidence that TRP-4 is an essential pore-forming subunit of the mechanotransduction channel in CEP.

DISCUSSION

TRP Family Channels Can Play a Direct Role in Mechanosensation

In the current report, to overcome the relative difficulty of characterizing mechanotransduction channels in vitro, we turned to the nematode *C. elegans,* an in vivo system that allowed us to record MRCs in vivo and to manipulate them with molecular genetic tools. We addressed the highly controversial role of TRP channels in mechanotransduction. Our results indicate that the TRPN channel TRP-4 functions as a pore-lining subunit of a mechanotransduction channel in vivo. Importantly, the short latency and rapid activation kinetics of TRP-4 currents are consistent with the view that this type of channels is gated by mechanical forces. Thus, TRP channels can play a direct role in mechanotransduction.

It remains unclear what contributed to the conflicting results with respect to the role of TRP channels in mechanosensation. One possibility is that when expressed in vitro, TRP channels may interact with endogenous mechanotransduction channels and/or other channel-interacting proteins (Gottlieb et al., 2008). Different heterologous systems may express different sets of mechanotransduction channels and interacting-proteins. One recent report has elegantly clarified the role of the polycystin TRP channel TRPP2/PKD2 in mechanosensation by demonstrating that TRPP2 regulates mechanosensation not by acting

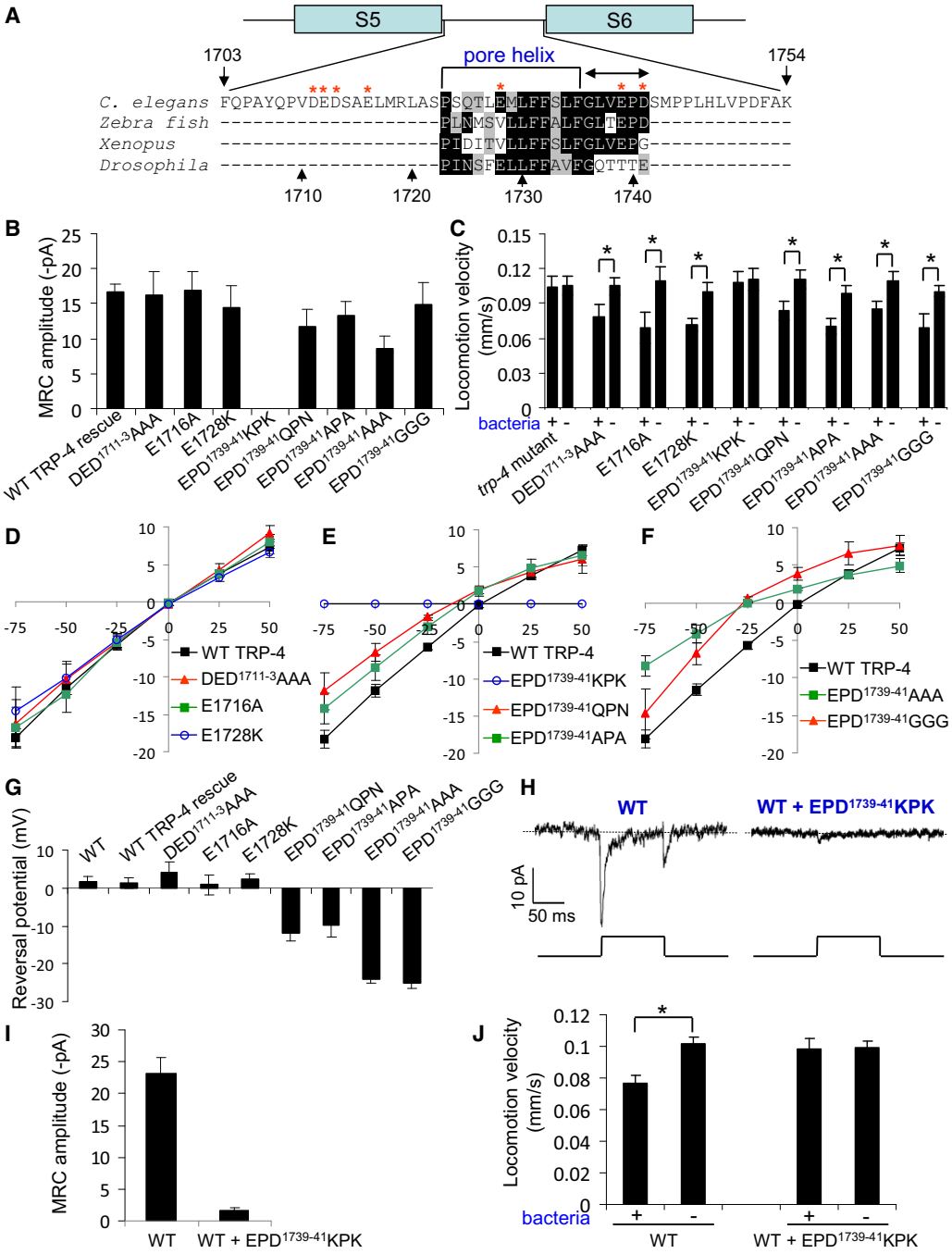

Figure 7. TRP-4 Is an Essential Pore-Forming Subunit of the Mechanotransduction Channel in CEP

(A) Sequence alignment of the putative pore region of TRP-4 and its homologs. The bracket denotes the putative pore helix that is predicted to form an alpha helix structure by the program PSIPRED. Other programs (e.g., Prof and SSpro) also yield a similar prediction. The double-headed arrow indicates the putative selectivity filter. The sequences outside the pore region but within the S5-S6 linker area are not shown for other organisms as they do not show much homology. Asterisks in red mark the negatively charged residues D and E that were mutated in various TRP-4 mutant forms. TRP-4 homologs are found in *Xenopus*, zebrafish, and *Drosophila* but not higher vertebrates.

(B) MRC amplitude in CEP recorded from transgenic worms expressing various mutant forms of TRP-4. Wild-type TRP-4 rescue data from 6D are also included. All transgenes were expressed in the *trp-4(sy695)* mutant background. It should be noted that the expression level of different transgenes may vary and such variation may contribute to the difference in the amplitude of MRCs carried by different forms of TRP-4. Displacement: 4 μm. $n \geq 5$.

(C) Rescue of the basal slowing behavioral response by transgenes encoding various mutant forms of TRP-4. All transgenes were expressed in the *trp-4(sy695)* mutant background. $n \geq 10$. *$p < 0.05$ (t test).

(D–F) I-V relations. Wild-type TRP-4 was included in each panel for comparison.

as a mechanotransduction channel but rather by modulating the activity of a native mechanotransduction channel of unknown molecular identity (Sharif-Naeini et al., 2009).

C. elegans Offers a Valuable Model to Interrogate the Role of TRP Family Channels in Mechanosensation

C. elegans represents a nice system to study mechanosensation in vivo, due to its amenability to genetic manipulation and short generation time. In particular, the ability to record MRCs in vivo by whole-cell recording, in conjunction with the availability of facile genetic tools, offers a powerful means to dissect the molecular underpinnings of mechanotransduction at the organismal level. The worm genome encodes 17 TRP family members that cover all of the seven TRP subfamilies (Kahn-Kirby and Bargmann, 2006; Xiao and Xu, 2009). These genes are widely expressed in the nervous system, as well as in some nonexcitable cells (Kahn-Kirby and Bargmann, 2006; Xiao and Xu, 2009). In addition to dopamine neurons, a number of other ciliated neurons have also been categorized as mechanosensory neurons in hermaphrodites and males, and they all express TRP family genes (Kahn-Kirby and Bargmann, 2006; Xiao and Xu, 2009). For example, The TRPV channels OSM-9 and OCR-2 and the TRPA channel TRPA-1 have been implicated in mechanosensation (Colbert et al., 1997; Kindt et al., 2007b; Tobin et al., 2002). Notably, the mammalian TRPA1 and TRPV channels have also been implicated in mechanosensation, but whether these channels play a direct or indirect role in mechanosensation has become a subject of intense debate (Bautista et al., 2006; Christensen and Corey, 2007; Kwan et al., 2006; Sharif-Naeini et al., 2008). It will be very interesting to address this question in *C. elegans*.

Like voltage, ligand and temperature-gated ion channels, the exact gating mechanisms for mechanically gated channels are not clear. Two primary models have been proposed: the membrane stretch model and the tether model in which membrane stretch and protein tether pulls open the transduction channel, respectively (Christensen and Corey, 2007). TRP-4 may be gated by one of these mechanisms. It is also possible that these two mechanisms are not mutually exclusive. Notably, the cilium of CEP is anchored to the overlying cuticle through a small nubbin (Figure 1A). This anchor may stretch the cilium membrane upon mechanical deflection. Alternatively, this anchor may act in a manner analogous to the tip link found in vertebrate hair cells to pull open TRP-4. Like many ion channels, some auxiliary subunits may work in concert with TRP-4 to facilitate channel gating. One such example is the MEC-4/MEC-10/MEC-2/MEC-6 mechanotransduction channel complex (Bounoutas and Chalfie, 2007). In this complex, MEC-4 and MEC-10 line the channel pore while MEC-2 and MEC-6 facilitate the gating of the MEC-4/MEC10 channel by linking it to the cytoskeleton and extracellular matrix, respectively (Bounoutas and Chalfie, 2007). However, whether TRP-4 also functions in a channel complex remains to be determined.

Concluding Remarks

In mammals, most of the cell types that have thus far been examined show some form of mechanosensitivity with diverse properties (Sachs, 1991). However, very little is known about the underlying transduction channels in mammalian cells. In fact, among the four major classes of ion channels (i.e., voltage, ligand, mechanically, and temperature gated), mechanotransduction channels probably represent the largest group of channels whose molecular identities are largely unknown. There are at least 28 TRP family members in vertebrates (Nilius and Voets, 2005; Ramsey et al., 2006; Venkatachalam and Montell, 2007). Our work raises the possibility that other TRP channels may also function as mechanotransduction channels. As TRP proteins often interact to form heteromeric channels (Strubing et al., 2001; Xu et al., 1997), they can potentially encode a large group of mechanotransduction channels with diverse biophysical properties and distinct biological functions.

EXPERIMENTAL PROCEDURES

Behavioral Analysis

The basal slowing response was recorded using an automated worm tracking system as previously described (Feng et al., 2006; Li et al., 2006). In brief, L4 hermaphrodites were picked 16 hr before tracking. Animals were tracked for 6 min on NGM plates spread with a thin layer of freshly grown OP50 bacteria or with supernatant from OP50 culture. For transgenic lines, only nonmosaic worms were selected for tracking. The last 4 min of tacking data were used to compute locomotion velocity.

Molecular Biology

trp-4 cDNA was inserted between the *dat-1* promoter and an SL2::YFP fragment. SL2 achieves a role analogous to that played by IRES in mammalian expression vectors. This strategy allows for simultaneous expression of TRP-4 and YFP in CEP from a single construct. All point mutations were introduced by site-directed mutagenesis (Quick change) and verified by sequencing the entire *trp-4* coding region. Transgenic lines were generated by directly injecting *trp-4* cDNA constructs into *trp-4(sy695)* mutant worms.

Electrophysiology

Whole-cell recordings were performed on an Olympus microscope (BX51WI) with an EPC-10 amplifier and the Patchmaster software (HEKA) using a protocol described previously (Brockie et al., 2001; Goodman et al., 1998; Liu et al., 2010; Richmond and Jorgensen, 1999; Ward et al., 2008). In brief, a glass stimulus probe was driven by a Piezo actuator (PI) mounted on a micromanipulator and triggered by the amplifier. Worms were glued to a sylgard-coated coverglass covered with bath solution, and a small piece of cuticle in the worm head was cut open and pinned down to the coverglass to expose the cell body of CEP. Caution was exercised to keep intact the nose tip where the cilium of CEP is housed. This preparation well preserved the function of CEP; however, it did not permit rapid exchange of bath solution surrounding the cilium where TRP-4 is localized (usually takes a couple of minutes to equilibrate). This limited our ability to test the effect of some "toxic" bath solutions

(G) Summary of reversal potential data. Wild-type TRP-4 and various mutant forms of TRP-4 were all expressed in the *trp-4(sy695)* mutant background. Data from wild-type worms were also shown for comparison. $n \geq 5$.

(H and I) The "pore-dead" mutant $EPD^{1739\text{-}41}KPK$ blocks endogenous MRCs in CEP of wild-type worms. The tiny remaining current may result from those very few homomeric wild-type TRP-4 channels that did not heteromerize with the mutant, assuming that TRP-4 functions as a tetramer. Wild-type data from 6D are also included. Displacement: 4 μm. $n \geq 6$.

(J) Wild-type worms expressing the "pore-dead" mutant form $EPD^{1739\text{-}41}KPK$ lack the basal slowing behavioral response. $n \geq 12$. *$p < 0.05$ (t test).

(e.g., Ca^{2+} only solution and Ca^{2+}-free solution) on reversal potential, as the patch was always lost before solution exchange completed. Thus, we were unable to determine the Ca^{2+} permeability of TRP-4. Perfusion of Gd^{3+} and La^{3+} (100 μM) can block CEP MRCs; however, as we were unable to wash out such an inhibitory effect (slow solution exchange) before losing the seal, it is unclear whether this effect is specific (data not shown).

The CEP neuron was identified by a yellow or red fluorescent protein marker expressed as a transgene driven by the *dat-1* promoter (Lints and Emmons, 1999). Recording pipettes were pulled from borosilicate glass. The bath solution contains 145 mM NaCl, 10 mM HEPES, 20 mM glucose, 1 mM $MgCl_2$, 1 mM $CaCl_2$, and 2.5 mM KCl (335 mOsm [pH adjusted to 7.3 with NaOH]). The pipette solution contains 145 mM CsCl, 10 mM HEPES, 20 mM glucose, 0.25 mM $CaCl_2$, and 5 mM EGTA, 5 mM ATP, 0.5 mM GTP (325 mOsm [pH adjusted to 7.2 with CsOH]). In "Cl^--free" solution, Cs-gluconate was used to replace CsCl. ATP and GTP were not essential for MRCs in CEP, but their inclusion prolonged the life of the patch. CsCl solution was used (unless otherwise indicated) to block K^+ currents, reducing noises during recording and also enabling I-V analysis of MRCs. Voltages were clamped at −75 mV. Current data were sampled at 20–40 kHz. Series resistance and membrane capacitance were both compensated during recording. Liquid junction potentials were also corrected.

To estimate the relative permeability P_{Cs+}/P_{Na+}, we used the following equation derived from the Goldman-Hodgkin-Katz model as previously described (Hille, 2001):

$$E_{rev} = \frac{RT}{zF} \ln \frac{P_{Na^+}[Na^+]_{out}}{P_{Cs^+}[Cs^+]_{in}}$$

where E_{rev} is the reversal potential of the current.

For nonstationary noise analysis, the variance values were plotted against mean current, and the data were fit with the equation as previously described (Hille, 2001):

$$\sigma^2(I) = iI - I^2/N$$

where σ^2 is the variance, i represents the single channel current, and N indicates the number of channels available for activation. This method works best for those channels that do not undergo desensitization to repeated stimuli. The single channel conductance was then calculated as:

$$\gamma = i/(V_m - E_{rev})$$

where V_m is the holding potential, and E_{rev} is the reversal potential of the current . Most, if not all, worm neurons are known to be nearly isopotential, thus voltage attenuation is minimal (Goodman et al., 1998).

SUPPLEMENTAL INFORMATION

Supplemental Information includes three figures and can be found with this article online at doi:10.1016/j.neuron.2010.06.032.

ACKNOWLEDGMENTS

We thank H. Xu and A. Kumar for comments on the manuscript and R. Xiao for sequence alignment and structural modeling. Some strains were obtained from the Caenorhabditis Genetics Center. J.G. and Z.X. received support from the Chinese 111 project (B06018). This work was supported by grants from the NIGMS and the Pew Scholar Program (X.Z.S.X.).

Accepted: June 16, 2010
Published: August 11, 2010

REFERENCES

Bautista, D.M., Jordt, S.E., Nikai, T., Tsuruda, P.R., Read, A.J., Poblete, J., Yamoah, E.N., Basbaum, A.I., and Julius, D. (2006). TRPA1 mediates the inflammatory actions of environmental irritants and proalgesic agents. Cell *124*, 1269–1282.

Bounoutas, A., and Chalfie, M. (2007). Touch sensitivity in Caenorhabditis elegans. Pflugers Arch. *454*, 691–702.

Brockie, P.J., Mellem, J.E., Hills, T., Madsen, D.M., and Maricq, A.V. (2001). The C. elegans glutamate receptor subunit NMR-1 is required for slow NMDA-activated currents that regulate reversal frequency during locomotion. Neuron *31*, 617–630.

Christensen, A.P., and Corey, D.P. (2007). TRP channels in mechanosensation: direct or indirect activation? Nat. Rev. *8*, 510–521.

Colbert, H.A., Smith, T.L., and Bargmann, C.I. (1997). OSM-9, a novel protein with structural similarity to channels, is required for olfaction, mechanosensation, and olfactory adaptation in Caenorhabditis elegans. J. Neurosci. *17*, 8259–8269.

Davies, A.G., Pierce-Shimomura, J.T., Kim, H., VanHoven, M.K., Thiele, T.R., Bonci, A., Bargmann, C.I., and McIntire, S.L. (2003). A central role of the BK potassium channel in behavioral responses to ethanol in C. elegans. Cell *115*, 655–666.

Feng, Z., Li, W., Ward, A., Piggott, B.J., Larkspur, E., Sternberg, P.W., and Xu, X.Z.S. (2006). A C. elegans model of nicotine-dependent behavior: regulation by TRP family channels. Cell *127*, 621–633.

Gillespie, P.G., and Walker, R.G. (2001). Molecular basis of mechanosensory transduction. Nature *413*, 194–202.

Goodman, M.B., Hall, D.H., Avery, L., and Lockery, S.R. (1998). Active currents regulate sensitivity and dynamic range in C. elegans neurons. Neuron *20*, 763–772.

Gottlieb, P., Folgering, J., Maroto, R., Raso, A., Wood, T.G., Kurosky, A., Bowman, C., Bichet, D., Patel, A., Sachs, F., et al. (2008). Revisiting TRPC1 and TRPC6 mechanosensitivity. Pflugers Arch. *455*, 1097–1103.

Hille, B. (2001). Ion Channels of Excitable Membranes, Third Edition (Sunderland, MA: Sinauer Associates, Inc.).

Honore, E., Patel, A.J., Chemin, J., Suchyna, T., and Sachs, F. (2006). Desensitization of mechano-gated K2P channels. Proc. Natl. Acad. Sci. USA *103*, 6859–6864.

Kahn-Kirby, A.H., and Bargmann, C.I. (2006). TRP channels in C. elegans. Annu. Rev. Physiol. *68*, 719–736.

Kindt, K.S., Quast, K.B., Giles, A.C., De, S., Hendrey, D., Nicastro, I., Rankin, C.H., and Schafer, W.R. (2007a). Dopamine mediates context-dependent modulation of sensory plasticity in C. elegans. Neuron *55*, 662–676.

Kindt, K.S., Viswanath, V., Macpherson, L., Quast, K., Hu, H., Patapoutian, A., and Schafer, W.R. (2007b). Caenorhabditis elegans TRPA-1 functions in mechanosensation. Nat. Neurosci. *10*, 568–577.

Kung, C., and Blount, P. (2004). Channels in microbes: so many holes to fill. Mol. Microbiol. *53*, 373–380.

Kwan, K.Y., Allchorne, A.J., Vollrath, M.A., Christensen, A.P., Zhang, D.S., Woolf, C.J., and Corey, D.P. (2006). TRPA1 contributes to cold, mechanical, and chemical nociception but is not essential for hair-cell transduction. Neuron *50*, 277–289.

LeMasurier, M., and Gillespie, P.G. (2005). Hair-cell mechanotransduction and cochlear amplification. Neuron *48*, 403–415.

Li, W., Feng, Z., Sternberg, P.W., and Xu, X.Z.S. (2006). A C. elegans stretch receptor neuron revealed by a mechanosensitive TRP channel homologue. Nature *440*, 684–687.

Lints, R., and Emmons, S.W. (1999). Patterning of dopaminergic neurotransmitter identity among Caenorhabditis elegans ray sensory neurons by a TGFbeta family signaling pathway and a Hox gene. Development *126*, 5819–5831.

Liu, J., Ward, A., Gao, J., Dong, Y., Nishio, N., Inada, H., Kang, L., Yu, Y., Ma, D., Xu, T., et al. (2010). C. elegans phototransduction requires a G protein–dependent cGMP pathway and a taste receptor homolog. Nat. Neurosci. *13*, 715–722.

Mederos y Schnitzler, M., Storch, U., Meibers, S., Nurwakagari, P., Breit, A., Essin, K., Gollasch, M., and Gudermann, T. (2008). Gq-coupled receptors as

mechanosensors mediating myogenic vasoconstriction. EMBO J. *27*, 3092–3103.

Montell, C. (2005). The TRP superfamily of cation channels. Sci. STKE *2005*, re3.

Montell, C., and Rubin, G.M. (1989). Molecular characterization of the Drosophila trp locus: a putative integral membrane protein required for phototransduction. Neuron *2*, 1313–1323.

Nilius, B., and Voets, T. (2005). TRP channels: a TR(I)P through a world of multifunctional cation channels. Pflugers Arch. *451*, 1–10.

O'Hagan, R., Chalfie, M., and Goodman, M.B. (2005). The MEC-4 DEG/ENaC channel of Caenorhabditis elegans touch receptor neurons transduces mechanical signals. Nat. Neurosci. *8*, 43–50.

Owsianik, G., Talavera, K., Voets, T., and Nilius, B. (2006). Permeation and selectivity of TRP channels. Annu. Rev. Physiol. *68*, 685–717.

Perkins, L.A., Hedgecock, E.M., Thomson, J.N., and Culotti, J.G. (1986). Mutant sensory cilia in the nematode Caenorhabditis elegans. Dev. Biol. *117*, 456–487.

Ramsey, I.S., Delling, M., and Clapham, D.E. (2006). An introduction to TRP channels. Annu. Rev. Physiol. *68*, 619–647.

Richmond, J.E., and Jorgensen, E.M. (1999). One GABA and two acetylcholine receptors function at the C. elegans neuromuscular junction. Nat. Neurosci. *2*, 791–797.

Sachs, F. (1991). Mechanical transduction by membrane ion channels: a mini review. Mol. Cell. Biochem. *104*, 57–60.

Sawin, E.R., Ranganathan, R., and Horvitz, H.R. (2000). C. elegans locomotory rate is modulated by the environment through a dopaminergic pathway and by experience through a serotonergic pathway. Neuron *26*, 619–631.

Sharif-Naeini, R., Dedman, A., Folgering, J.H., Duprat, F., Patel, A., Nilius, B., and Honore, E. (2008). TRP channels and mechanosensory transduction: insights into the arterial myogenic response. Pflugers Arch. *456*, 529–540.

Sharif-Naeini, R., Folgering, J.H., Bichet, D., Duprat, F., Lauritzen, I., Arhatte, M., Jodar, M., Dedman, A., Chatelain, F.C., Schulte, U., et al. (2009). Polycystin-1 and −2 dosage regulates pressure sensing. Cell *139*, 587–596.

Sidi, S., Friedrich, R.W., and Nicolson, T. (2003). NompC TRP channel required for vertebrate sensory hair cell mechanotransduction. Science *301*, 96–99.

Strubing, C., Krapivinsky, G., Krapivinsky, L., and Clapham, D.E. (2001). TRPC1 and TRPC5 form a novel cation channel in mammalian brain. Neuron *29*, 645–655.

Tobin, D., Madsen, D., Kahn-Kirby, A., Peckol, E., Moulder, G., Barstead, R., Maricq, A., and Bargmann, C. (2002). Combinatorial expression of TRPV channel proteins defines their sensory functions and subcellular localization in C. elegans neurons. Neuron *35*, 307–318.

Venkatachalam, K., and Montell, C. (2007). TRP channels. Annu. Rev. Biochem. *76*, 387–417.

Walker, R.G., Willingham, A.T., and Zuker, C.S. (2000). A Drosophila mechanosensory transduction channel. Science *287*, 2229–2234.

Ward, A., Liu, J., Feng, Z., and Xu, X.Z. (2008). Light-sensitive neurons and channels mediate phototaxis in C. elegans. Nat. Neurosci. *11*, 916–922.

Watanabe, H., Vriens, J., Prenen, J., Droogmans, G., Voets, T., and Nilius, B. (2003). Anandamide and arachidonic acid use epoxyeicosatrienoic acids to activate TRPV4 channels. Nature *424*, 434–438.

Xiao, R., and Xu, X.Z. (2009). Function and regulation of TRP family channels in C. elegans. Pflugers Arch. *458*, 851–860.

Xu, X.Z.S., Li, H.S., Guggino, W.B., and Montell, C. (1997). Coassembly of TRP and TRPL produces a distinct store-operated conductance. Cell *89*, 1155–1164.

Yin, J., and Kuebler, W.M. (2010). Mechanotransduction by TRP channels: general concepts and specific role in the vasculature. Cell Biochem. Biophys. *56*, 1–18.